White Dwarfs as Probes of Fundamental Physics and Tracers of Planetary, Stellar, and Galactic Evolution
Proceedings IAU Symposium No. 357, 2019
****NAME OF EDITORS****

DOI: 00.0000/X000000000000000X

White-dwarf asteroseismology: an update

Alejandro H. Córsico[1,2]

[1]Facultad de Ciencias Astronómicas y Geofísicas, Universidad Nacional de La Plata, Paseodel Bosque s/n, (1900) La Plata, Argentina,
[2] Instituto de Astrofísica de La Plata, IALP (CCT La Plata), CONICET-UNLP
email: acorsico@fcaglp.unlp.edu.ar

Abstract. The vast majority of stars that populate the Universe will end their evolution as white-dwarf stars. Applications of white dwarfs include cosmochronology, evolution of planetary systems, and also as laboratories to study non-standard physics and crystallization. In addition to the knowledge of their surface properties from spectroscopy combined with model atmospheres, the global pulsations that they exhibit during several phases of their evolution allow spying on the deep interior of these stars. Indeed, by means of asteroseismology, an approach based on the comparison between the observed pulsation periods of variable white dwarfs and the periods predicted by representative theoretical models, we can infer details of the internal chemical stratification, the total mass, and even the stellar rotation profile and strength of magnetic fields. In this article, we review the current state of the area, emphasizing the latest findings provided by space-mission data.

Keywords. stars: oscillations, stars: evolution, white dwarfs

1. Introduction

White-dwarf stars constitute the end fate of ~ 97 % of all the stars that populate the Universe, included our Sun. Indeed, all the stars with a mass lower than $\sim 8 M_{\odot}$ in the Main Sequence (MS) will passively end their lives as white dwarfs. The reader interested in details about the formation and evolution of white dwarfs can consult the review article by Althaus et al. (2010). Here, we will only give a brief review of the main characteristics of these stars. White dwarfs are compact stars, characterized by mean densities of the order of $\overline{\rho} \sim 10^6$ gr/cm^3 (in comparison, $\overline{\rho_{\odot}} = 1.41$ gr/cm^3) and radii of roughly $R_{\star} \sim 0.01 R_{\odot}$. They cover a wide interval of surface temperatures ($4000 \lesssim T_{\rm eff} \lesssim 200\,000$ K) and, consequently, a vast range of luminosities ($0.0001 \lesssim L_{\star}/L_{\odot} \lesssim 1000$). The mass distribution of white dwarfs is characterized by a very pronounced peak at $M_{\star} \sim 0.6 M_{\odot}$ (the average mass), although the mass range is quite wide ($0.15 \lesssim M_{\star}/M_{\odot} \lesssim 1.3$). White dwarfs with masses in the range $0.45 \lesssim M_{\star}/M_{\odot} \lesssim 1.0$ likely have cores made of ^{12}C and ^{16}O, while the less massive ones ($M_{\star}/M_{\odot} \lesssim 0.45$) probably harbor ^{4}He cores, and the most massive ones ($M_{\star}/M_{\odot} \gtrsim 1.0$) could have cores made of ^{16}O, ^{20}Ne and ^{24}Mg. Due to the high densities characterizing white dwarfs, the equation of state that governs most of the structure of a white dwarf is that corresponding to a Fermi gas of degenerate electrons, which provide most of the pressure. In turn, the non-degenerate ions contribute to the mass of the star and the heat content accumulated during the previous evolutionary stages. Loosely speaking, the evolution of a white dwarf consists in a gradual cooling, during which the energy sources of nuclear reactions are irrelevant, although there are some exceptions, such as very hot pre-white dwarfs, extremely low-mass (ELM) white dwarfs, and average-mass white dwarfs coming from low-metallicity progenitors.

By virtue of the high surface gravities ($\log g \sim 8$ [cgs]), the different chemical species

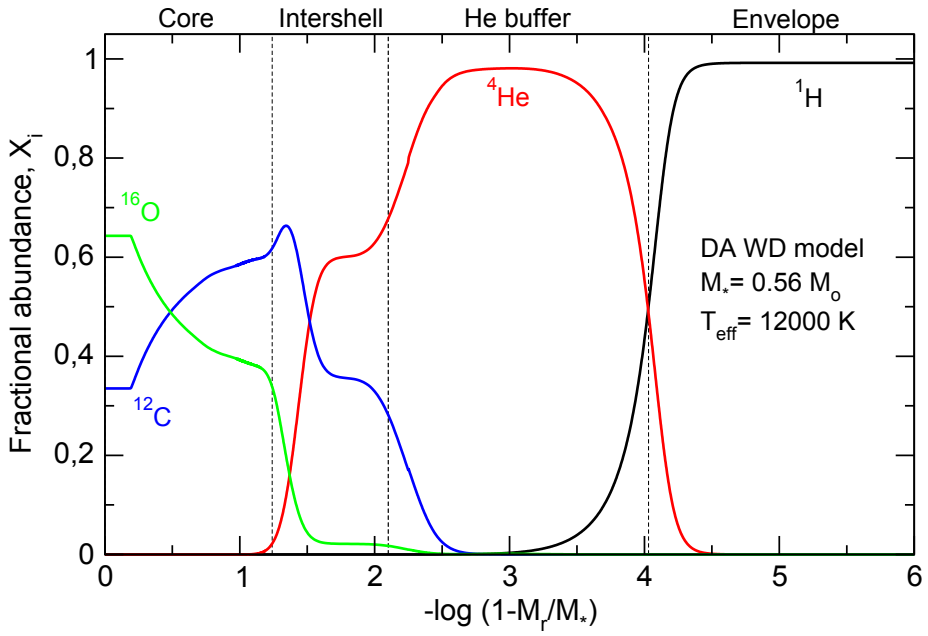

Figure 1. Internal chemical structure of a typical DA white dwarf model with $M_\star = 0.56 M_\odot$, $T_{\rm eff} \sim 12\,000$ K, and H envelope thickness of $\log(M_{\rm H}/M_\star) \sim -4$, resulting from the complete evolution of a single $1 M_\odot$ progenitor from the ZAMS to the white dwarf stage. Plotted is the mass fraction ($X_{\rm i}$) of ^{16}O (green), ^{12}C (blue), ^{4}He (red), and ^{1}H (black), in terms of the outer mass fraction coordinate. The centre of the star is at $-\log(1 - M_r/M_\star) = 0$. We separate with vertical dashed lines four different parts of the internal chemical structure of the model, the origin and the uncertainties of which are described in the text.

in these stars are well separated due to the effect of gravitational settling. According to the dominant chemical species on the surface of white dwarfs, they are classified into two main groups, those of the spectral type DA ($\sim 80\%$ of the total, atmospheres rich in H) and those of spectral type DB ($\sim 15\%$ of the total, atmospheres rich in He). Figure 1 shows the stratified chemical structure of a DA white dwarf model as a function of the outer mass coordinate. This coordinate strongly amplifies the outer regions of the star. As can be seen, 99% of the total mass of the star $[-\log(1 - M_r/M_\star) \lesssim 2]$ is composed mostly of C and O, the mass of the He layer being $M_{\rm He} \lesssim 0.01 M_\star$ and the mass of the H envelope being $M_{\rm H} \lesssim 0.0001 M_\star$. For illustrative purposes, we have divided the chemical structure of the star into four parts: the core, the intershell region, the He-buffer, and the H envelope. In Table 1, we include a short account of the origin and the uncertainties playing a role at each part of the chemical structure (see, for details, Córsico et al. 2019a).

Since white dwarfs are very old objects, with ages of the order of $\tau \sim 10^9 - 10^{10}$ years, they convey extremely valuable information about the evolution of stars "from the cradle to the grave", and about the rate of stellar formation along the complete history of our Galaxy. The study of white dwarfs has many applications to several fields. One one hand, they can provide an estimate of the age of stellar populations like open and globular clusters, and the halo and the galactic disk, by using the luminosity function of white dwarfs (see, for instance, García-Berro et al. 2010). On the other hand, due to the existence of a mass limit for white dwarfs (the Chandrasekhar mass), they are of utmost relevance as progenitors of supernovae of type Ia, and also cataclysmic variables like novae, that

Table 1. The different parts of the chemical structure (first row), their origin (second row), and their uncertainties (third row), corresponding to the DA white dwarf model shown in Fig. 1.

	Core	Intershell	He buffer	Envelope
Origin	The result of He-core burning and the following steady He burning	Built up during the TP-AGB phase	Shaped by gravitational settling. Prior H burning	Shaped by gravitational settling. Primordial H
Uncertainties	$^{12}C(\alpha,\gamma)^{16}O$ reaction rate, extra-mixing	Number of TPs, extra-mixing rotation (?)	Number of TPs, IFM relationship	Metallicity, C dredge-up, late He flashes

involve very energetic events ($E \sim 10^{44} - 10^{51}$ erg) of mass transfer onto the white dwarf surface from its companion star. Finally, by virtue of the extreme conditions of pressure and density prevailing inside white dwarfs, they allow the investigation of phenomena such as crystallization due to Coulomb interactions, the assessment of constraints on fundamental particles like axions and neutrinos, the variation of fundamental constants, etc. Classically, the approaches employed to study white dwarfs have been spectroscopy, photometry and astrometry, that allow us to infer the effective temperature, surface gravity and composition, parallaxes and distances, etc. Of particular interest in this article is the technique named "asteroseismology", that allows us to extract information of the *interior* of stars by studying how they pulsate. In the next section we provide a brief description of this technique applied to pulsating white-dwarf stars.

2. Stellar pulsations and white-dwarf asteroseismology

Asteroseismology is based on the well-known physical principle establishing that *"studying how a system vibrates in its normal modes allows us to infer its mechanical properties"*. In the case of stars, the vibrations are global pulsations that allow us to "see" the sub-photosferic layers, otherwise inaccessible by means of classical techniques†. Basically, asteroseismology consists in the comparison of theoretical periods of stellar models with the periods observed in real pulsating stars. In the case of white-dwarf asteroseismology, there are other tools to extract information for several quantities —in particular the stellar mass— on the basis of the asymptotic behavior of g (gravity) modes of high radial order. These tools will be described in Section 2.3. White-dwarf asteroseismology allows us to derive information about the stellar mass, the chemical stratification, the core chemical composition, the existence and strength of magnetic fields, the properties pf stellar rotation, the physics of convection, etc. Very detailed reports about white-dwarf asteroseismology can be found in the review articles by Fontaine & Brassard (2008); Winget & Kepler (2008); Althaus et al. (2010) and Córsico et al. (2019a).

2.1. *A little bit on nonradial stellar pulsations*

Stellar pulsations are eigenmodes of the stars that can be thought of as standing waves in 3 dimensions. Each star has a unique spectrum of discrete eigenfrequencies, the natural frequencies of the star, that is set by its internal structure, mass, effective temperature, radius, etc. In a sense, these natural frequencies are like the "fingerprints" of the star. The eigenfrequencies are associated with eigenfunctions that provide the spatial variation of the different physical parameters of the star when it pulsates. In white-dwarf stars,

† The only alternative way to obtain direct information from the stellar interior is through neutrinos, which escape from the depths of the stars without interacting with matter.

the frequency spectrum of pulsations is extremely sensitive to the details of the internal chemical stratification. Pulsations in stars can be radial, which retain the spherical symmetry (Cepheids, RR Lyrae, Miras, etc). Radial pulsations are a particular case of a very general class of oscillatory movements, called nonradial pulsations. The latter do not preserve the spherical symmetry. Nonradial pulsations are routinely detected in the Sun, and also in variable solar-type stars, red giants, δ Scuti, γ Doradus, β Cephei, SPB, WR, sdB, white dwarfs and pre-white dwarf stars. The detection of nonradial pulsations has experienced an unprecedented flourishing in the last years thanks to the advent of the space missions, such as MOST (Walker et al. 2003), CoRoT (Baglin et al. 2009), *Kepler* (Borucki et al. 2010) and K2 (Howell et al. 2014) —which have already ended— the TESS (Transiting Exoplanet Survey Satellite) mission (Ricker et al. 2015) —that is currently working— and the future missions Cheops (Moya et al. 2018) and Plato (Piotto 2018), among others.

In the frame of the linear theory, that assumes small amplitudes of pulsation, the deformations of a star when it pulsates in spheroidal modes are specified by the Lagrangian displacement vector (Unno et al. 1989):

$$\vec{\xi}_{k\ell m} = \left(\vec{\xi}_r, \vec{\xi}_\theta, \vec{\xi}_\phi\right)_{k\ell m} \tag{2.1}$$

where the components in spherical coordinates are:

$$\vec{\xi}_r = \xi_r(r) Y_\ell^m(\theta,\phi) e^{i\sigma t} \vec{e}_r \tag{2.2}$$

$$\vec{\xi}_\theta = \xi_h(r) \frac{\partial Y_\ell^m}{\partial \theta} e^{i\sigma t} \vec{e}_\theta \tag{2.3}$$

$$\vec{\xi}_\phi = \xi_h(r) \frac{1}{\sin\theta} \frac{\partial Y_\ell^m}{\partial \phi} e^{i\sigma t} \vec{e}_\phi \tag{2.4}$$

Here, $Y_\ell^m(\theta,\phi)$ are the spherical harmonics, σ is the pulsation frequency, and $\xi_r(r)$ y $\xi_h(r)$ are the radial and horizontal eigenfunctions, respectively. Each eigenmode has a sinusoidal temporal dependence, an angular dependence by means of spherical harmonics, and a radial dependence given through the radial and horizontal eigenfunctions, which must inevitably be obtained (for realistic star models) through the numerical resolution of the differential equations of stellar pulsations (see Unno et al. 1989). Pulsation modes are characterized by three "quantum numbers": *(i)* harmonic degree $\ell = 0, 1, 2, 3, \cdots, \infty$, that represents $(\ell - m)$ nodal lines (parallels) on the stellar surface, *(ii)* azimuthal order $m = -\ell, \cdots, -2, -1, 0, +1, +2, \cdots, +\ell$, that represents m nodal lines (meridians) on the stellar surface, and *(iii)* the radial order $k = 0, 1, 2, 3, \cdots, \infty$, that represents concentric spherical nodal surfaces on which the fluid displacement is null. Within the set of spheroidal modes†, there are two families of modes that differ according to the dominant restoring force. The p (pressure) modes, on one hand, involve large variations of pressure and displacements mostly radial, compressibility being the dominant restoring force. They are characterized by short periods (high frequencies). The g (gravity) modes, on the other hand, are associated with small variations of pressure and large tangential displacements. In this case, the restoring force is gravity through buoyancy, and the modes are characterized by long periods (small frequencies). These are the modes usually detected in white dwarfs. In the case in which $\ell > 1$, there exist a third sub-class of modes, the

† Spheroidal modes are characterized by $(\vec{\nabla} \times \vec{\xi})_r = 0$ and $\sigma^2 = 0$, where $\vec{\xi}$ is the Lagrangian displacement vector and σ the pulsation frequency (Unno et al. 1989).

f modes. They have intermediate characteristics between those of the p and g modes, and do not have radial nodes ($k = 0$), except for stellar models with very high central densities.

2.2. *White-dwarf pulsations*

2.2.1. *A brief historical account*

The first theoretical hints of pulsations in white dwarfs were revealed by the pioneering work of Sauvenier-Goffin (1949) and Ledoux & Sauvenier-Goffin (1950), who found instability in radial ($\ell = 0$) modes with periods of ~ 10 s due to hydrogen nuclear burning. These periods were not detected at that time, and this led to the conclusion that H burning is not the source of energy in a white dwarf, and allowed Mestel (1952) to elaborate his theory of cooling. The first pulsating white dwarf, HL Tau 76, was discovered by Landolt (1968), with a detected period of ~ 740 s, too long as to be due to a radial mode (Faulkner & Gribbin 1968; Ostriker & Tassoul 1968). Two additional pulsating white dwarfs, G44−32 (600-800 s) and R548 (200-300 s) (Lasker & Hesser 1969, 1971) were discovered shortly after, but again, the periods measured were too long as to be associated with radial modes. The first demonstration that the periods detected in these white dwarfs were due to nonradial g modes came from Warner & Robinson (1972) and Chanmugam (1972), in agreement with the theoretical work of Baglin (1969) and Harper & Rose (1970). An additional hint that these periods were due to nonradial modes came from the detection of rotational splitting in the observed frequencies (Robinson et al. 1976), since radial-mode frequencies do not exhibit splitting due to rotation. A definitive proof of the nonradial g-mode nature of the periods of pulsating white dwarfs was provided by the important work of McGraw (1979), who confirmed that the variability is due to changes in surface temperature and not to changes of the radius, which is typical of g modes. Finally, Robinson et al. (1982) demonstrated that the variations in the stellar radius are quite small ($\Delta R_\star \sim 10^{-5} R_\star$), and that the changes in effective temperature ($\Delta T_{\rm eff} \sim 200$ K) is what matters most in the pulsations of white dwarfs.

2.2.2. *The present situation*

Currently, it is a well established fact that, along their evolution, white dwarfs go through at least one stage of pulsation instability in which they become pulsating variable stars, showing light curves with variations in the optical and in the far UV parts of the electromagnetic spectrum (Winget & Kepler 2008; Fontaine & Brassard 2008; Althaus et al. 2010; Córsico et al. 2019a). The changes in brightness, with amplitudes between 0.001 mmag and 0.4 magnitudes, are due to g modes with harmonic degree $\ell = 1, 2$. In general terms, g modes in white dwarfs probe the envelope regions, due to the very low values of the Brunt-Väisälä frequency (the critical characteristic frequency for the g-mode spectrum) in the core regions. This is contrary to what happens in normal (non-degenerate) pulsating stars. At present, more than 350 pulsating white dwarfs and pre-white dwarfs have been discovered through observations from Earth, in their great majority extracted from the Sloan Digital Sky Survey (SDSS), and in the last years also through space missions such as the already finished *Kepler*/K2 Mission, and currently by TESS (Córsico et al. 2019a). Pulsating white dwarfs exhibit a wide variety of light curves, some sinusoidal and with small amplitudes, others nonlinear and with large amplitudes. They are multimodal pulsating stars (they pulsate in more than one period), and frequently exhibit harmonics and linear combinations of eigenfrequencies that are not related to genuine modes of pulsation, but instead to nonlinear effects. At present, there are six classes of confirmed pulsating white dwarfs and pre-white dwarfs known

Table 2. Properties of the different sub-classes of variable pulsating white dwarfs and pre-white dwarfs, sorted by decreasing effective temperature. The tentative classes of pulsators are labeled with a question mark in parentheses.

Class	Year of disc. (#)	$T_{\rm eff}$ [$\times$ 1000 K]	$\log g$ [C.G.S.]	Periods [s]	Amplitudes [mag]	Main surface composition
GW Vir (PNNV)	1984 (10)	$100-180$	$5.5-7$	$420-6000$	$0.01-0.15$	He, C, O
GW Vir (DOV)	1979 (9)	$80-100$	$7.3-7.7$	$300-2600$	$0.02-0.1$	He, C, O
Hot DAV (?)	2013 (3)	$30-32.6$	$7.3-7.8$	$160-705$	$0.001-0.015$	H
V777 Her (DBV)	1982 (27)	$22.4-32$	$7.5-8.3$	$120-1080$	$0.05-0.3$	He (H)
DQV (?)	2008 (6)	$19-22$	$8-9$	$240-1100$	$0.005-0.015$	He, C
GW Lib	1998 (20)	$10.5-16$	$8.35-8.7$	$100-1900$	$0.007-0.07$	H, He
ZZ Cet (DAV)	1968 (260)	$10.4-12.4$	$7.5-9.1$	$100-1400$	$0.01-0.3$	H
pre-ELMV	2013 (5)	$8-13$	$4-5$	$300-5000$	$0.001-0.05$	He, H
ELMV	2012 (11)	$7.8-10$	$6-6.8$	$100-6300$	$0.002-0.044$	H

(ZZ Ceti or DAV stars, GW Lib stars, V777 Her or DBV stars, GW Vir stars, ELMV stars and pre-ELMV stars) and two tentative classes of white-dwarf pulsators, that need confirmation (hot DAV stars and DQV stars). In Table 2 we show in a compact way the main characteristics of these families of pulsating white dwarfs and pre-white dwarfs, while in Figure 2 we show their location in the $\log T_{\rm eff} - \log g$ diagram (details can be found in Córsico et al. 2019a). In Table 2, the second column indicates the discovery year of the first object of each class and number of known objects at the date of writing this article (November 2019), the third column shows the range of effective temperatures at which they are detected (instability strip), the fourth column provides the range of surface gravity, the fifth column indicates the range of periods detected, the sixth column contains the range of amplitudes of the variations in the light curves, and the seventh column shows the surface composition. Pulsation periods are usually between $\sim$ 100 s and $\sim$ 1400s, although PNNVs and ELMVs exhibit much longer periods, up to $\sim$ 6300 s. Interestingly, the periods of g modes of white dwarfs are of the same order of magnitude as the periods of p modes in non-degenerate pulsating stars.

2.3. *The tools of white-dwarf asteroseismology*

The tools employed in asteroseismology of pulsating white dwarf stars have been described in several review articles (Winget & Kepler 2008, Fontaine & Brassard 2008, Althaus et al. 2010). Here, we will focus on the information that the existence of a constant (or nearly constant) period separation among the periods observed for a given star can give about the stellar mass, in particular in the case of GW Vir stars and DBVs. Also, we will describe the search for asteroseismological models that replicate the individual observed periods in real stars, that is, the period-to-period fits. Finally, we will revise the information about the stellar rotation that is possible to extract from the frequency splittings.

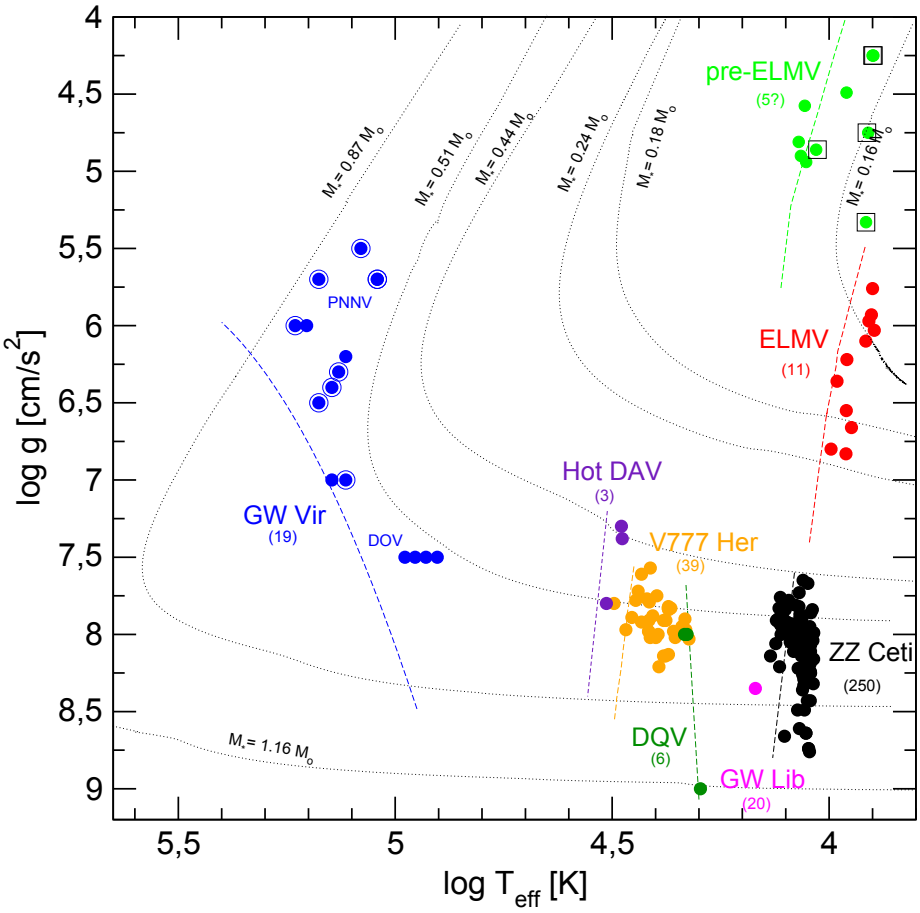

Figure 2. Confirmed and tentative sub-classes of pulsating white-dwarf and pre-white-dwarf stars (circles of different colors) in the $\log T_{\rm eff} - \log g$ diagram (adapted from Córsico et al. 2019a). Stars emphasized with squares surrounding the light green circles can be identified as pre-ELMV stars as well as SX Phe and/or δ Scuti stars. GW Vir stars indicated with blue circles surrounded by blue circumferences are PNNVs. In the case of GW Lib stars, only the location of the prototypical object, GW Librae, has been included (magenta dot). Two post-VLTP (Very Late Thermal Pulse) evolutionary tracks for H-deficient white dwarfs (0.51 and $0.87 M_\odot$; Miller Bertolami & Althaus 2006), four evolutionary tracks of low-mass He-core H-rich white dwarfs (0.16, 0.18, 0.24, and $0.44 M_\odot$; Althaus et al. 2013), and one evolutionary track for ultra-massive H-rich white dwarfs (Camisassa et al. 2019) are plotted for reference. Dashed lines indicate the theoretical blue edge of the instability domains.

2.3.1. *Clues to the stellar mass from the period spacing*

For g-modes with high radial order k (long periods), the separation of consecutive periods ($|\Delta k| = 1$) becomes nearly constant at a value given by the asymptotic theory of nonradial stellar pulsations. Specifically, the asymptotic period spacing (Tassoul et al. 1990) is given by:

$$\Delta\Pi_\ell^{\rm a} = \Pi_0/\sqrt{\ell(\ell+1)}, \tag{2.5}$$

where

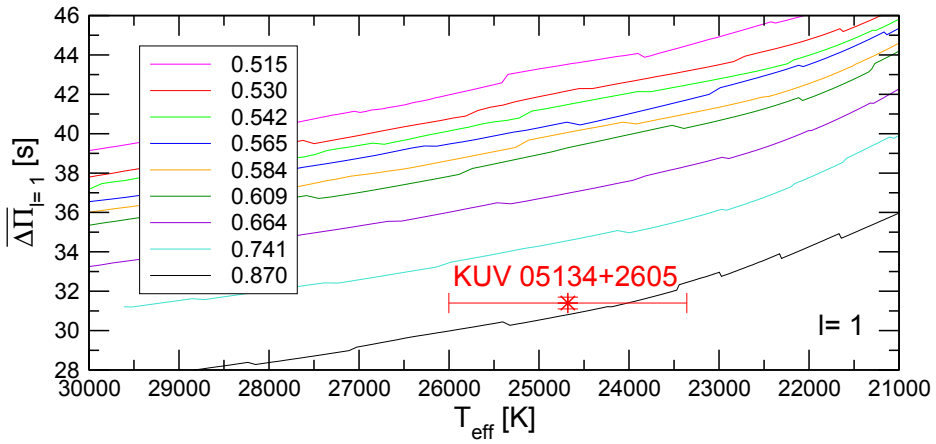

Figure 3. Average of the computed period spacings for $\ell = 1$ corresponding to DB white dwarf sequences with different stellar masses. The location of the target star KUV 05134+2605 is shown with a red star symbol ($T_{\rm eff}$ = 24 700 $\pm$ 1300 K) for each solution of observed mean period spacing, $\Delta\Pi_{\ell=1} = 31.4 \pm 0.3$ s. By simple linear interpolation, we found that the mass of the star according to its period spacing is $M_\star = 0.85 \pm 0.05 M_\odot$.

$$\Pi_0 = 2\pi^2 \left[\int_{r_1}^{r_2} \frac{N}{r} dr \right]^{-1}, \tag{2.6}$$

N being the Brunt-Väisälä frequency. This expression is rigorously valid for chemically homogeneous stars. In principle, one can compare the asymptotic period spacing computed from a grid of models with different masses and effective temperatures with the mean period spacing exhibited by the star, and then infer the value of the stellar mass. This method has been applied in numerous studies of pulsating PG 1159 stars (see, for instance, Córsico et al. 2007a,b, 2008, 2009, and references therein). For the method to be valid, the periods exhibited by the pulsating star must be associated with high order g modes, that is, the star must be within the asymptotic regime of pulsations. Furthermore, the interior of white-dwarf stars are supposed to be chemically stratified and characterized by strong chemical gradients built up during the progenitor star life. So, the direct application of the asymptotic period spacing to infer the stellar mass of white dwarfs is somewhat questionable. A better way to compare the models to the period spacing of the observed pulsation spectrum, is to calculate the average of the computed period spacings, using:

$$\overline{\Delta\Pi}(M_\star, T_{\rm eff}) = \frac{1}{(n-1)} \sum_{k}^{n-1} \Delta\Pi_k, \tag{2.7}$$

where $\Delta\Pi_k$ is the "forward" period spacing defined as $\Delta\Pi_k = \Pi_{k+1} - \Pi_k$, and n is the number of computed periods laying in the range of the observed periods. The theoretical period spacing of the models as computed through Eq. (2.5) and (2.7) share the same general trends (that is, the same dependence on $M_\star$ and $T_{\rm eff}$), although $\Delta\Pi_\ell^{\rm a}$ is usually somewhat higher than $\overline{\Delta\Pi}$, particularly for the case of low radial-order g modes. We can compare the measured mean period spacing of a given pulsating white dwarf with the average of the computed period spacings for several sequences with different stellar masses, by fixing the effective temperature and its uncertainties for the target star derived from spectroscopy. In this way, an estimate of the stellar mass can be obtained. As an

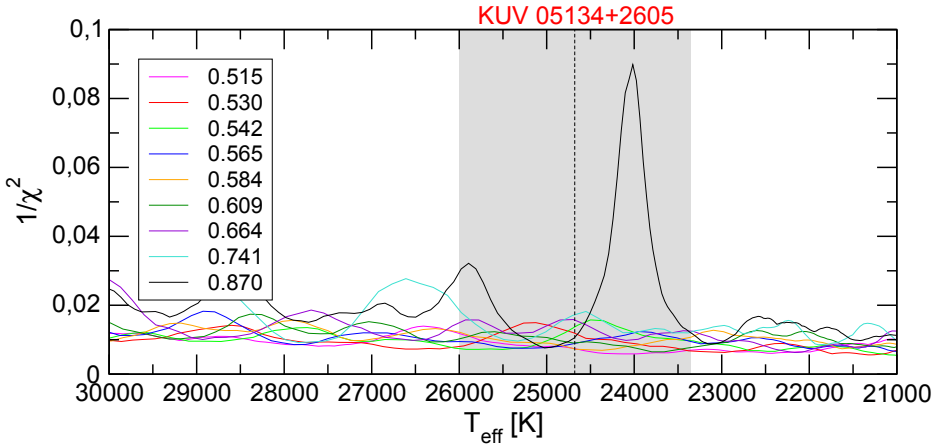

Figure 4. Inverse of the quality function of the period fit in terms of the effective temperature. The vertical gray strip indicates the spectroscopic $T_{\rm eff}$ of KUV 05134+2605 and its uncertainties ($T_{\rm eff} = 24\,680 \pm 1322$ K). The strong maximum in $(\chi^2)^{-1}$ corresponds to the best-fit model, with $M_\star = 0.870 M_\odot$ and $T_{\rm eff} = 23\,976$ K.

example of application, in Fig. 3 we show the run of the average of the computed period spacings [Eq. (2.7)] with $\ell = 1$, in terms of the effective temperature for a set of DB white dwarf evolutionary sequences. In the plot, we have included the measured period spacing for a DBV star, KUV 05134+2605 ($T_{\rm eff} = 24\,700 \pm 1300$ K and $\log g = 8.21 \pm 0.06$; Bergeron et al. 2011), whose period spectrum exhibits $\Delta\Pi_{\ell=1} = 31.4 \pm 0.3$ s. By means of a linear interpolation, we obtain the mass of the star according to its period spacing, $M_\star = 0.85 \pm 0.05 M_\odot$.

A cautionary word is necessary here. In the case of GW Vir stars and DBV stars, the period spacing is sensitive mostly to the stellar mass and effective temperature and very weakly to the thickness of the He envelope in the case of DBVs (see Tassoul et al. 1990) and the thickness of the C/O/He envelope in the case of the GW Vir stars (Kawaler, & Bradley 1994). In the case of ZZ Ceti stars, however, the period spacing depends on the stellar mass, the effective temperature, and the thickness of the H envelope with a comparable sensitivity. Consequently, the method is not —in principle— directly applicable to ZZ Ceti stars due to the intrinsic degeneracy of the dependence of $\Delta\Pi$ with the three parameters $M_\star$, $T_{\rm eff}$, and $M_{\rm H}$ (Fontaine & Brassard 2008). An illustration of this has been recently given in the asteroseismological study of ultra-massive ZZ Ceti stars by Córsico et al. (2019b).

2.3.2. *Constraints from period-to-period fits*

Another way to infer the stellar mass, along with the effective temperature and also many details of the internal structure of pulsating white dwarfs, is through their individual pulsation periods. In this approach, we seek a pulsation white dwarf model that best matches the pulsation periods of the target star. The goodness of the match between the theoretical pulsation periods (Π_k) and the observed individual periods ($\Pi_{{\rm obs},i}$) is measured by means of a quality function defined as:

$$\chi^2(M_\star, T_{\rm eff}) = \frac{1}{N} \sum_{i=1}^{N} \min[(\Pi_{{\rm obs},i} - \Pi_k)^2], \tag{2.8}$$

where N is the number of observed periods. The white dwarf model that shows the

lowest value of χ^2 is adopted as the "best-fit model" (see Córsico et al. 2007a,b, 2008, 2009, 2012; Bell et al. 2019). The quality of the period fits is assessed by means of the average of the absolute period differences, $\overline{\delta} = (\sum_{i=1}^{N} |\delta_i|)/N$, where $\delta_i = \Pi_{\rm obs,i} - \Pi_k$, and by the root-mean-square residual, $\sigma = \sqrt{(\sum |\delta_i|^2)/N} = \sqrt{\chi^2}$. Also, in order to have an indicator of the quality of the period fit, we can compute the Bayes Information Criterion (BIC; Koen, & Laney 2000):

$$\mathrm{BIC} = N_{\rm p} \left(\frac{\log N}{N} \right) + \log \sigma^2, \tag{2.9}$$

where $N_{\rm p}$ is the number of free parameters, and N the number of observed periods. The smaller the value of BIC, the better the quality of the fit. Following the same example of the previous section, in Fig. 4 we show the inverse of the quality function of the period fit for the DBV star KUV 05134+2605 in terms of the effective temperature. The vertical gray strip indicates the spectroscopic $T_{\rm eff}$ and its uncertainties. Clearly, the model that best reproduces the observed periods has a stellar mass of $0.87 M_{\odot}$ and an effective temperature $T_{\rm eff} \sim 24\,000$ K.

2.3.3. *Rotational splittings*

When a pulsating star is rotating, the frequencies of nonradial pulsation modes split into $2\ell + 1$ components, and their separation is proportional to the velocity of rotation of the star. In this way, when a pulsating white dwarf exhibits rotational splitting, it is possible to constrain its rotation period. If the rotation is slow and rigid, the rotation frequency Ω of the white dwarf is connected with the frequency splitting $\delta\nu$ through the coefficients $C_{k,\ell}$ —that depend on the details of the stellar structure— and the values of m $(-\ell, \cdots, -1, 0, +1, \cdots, +\ell)$, by means of the expression $\delta\nu = m(1 - C_{k,\ell})\ \Omega$ (Unno et al. 1989). Note that, when present, frequency splitting ($\ell = 1$: triplets, $\ell = 2$: quintuplets, etc) allows us to identify the harmonic degree ℓ and the azimuthal order m of the modes. Thanks to this effect, the rotation rate of many pulsating white dwarf stars has been measured (see next Section).

3. Recent findings

In this section, we describe the most recent results of white-dwarf asteroseismology. In particular, we will focus on outstanding findings that have been the result of uninterrupted observations from space, in particular, through the *Kepler*/K2 Mission. These findings would not have been possible through observations from the ground. We mainly describe the results from several relevant works that study the pulsation properties of V777 Her and ZZ Ceti stars from space-based observations. We also describe the first asteroseismological analysis carried out on the DBV star EC01585−1600 with the TESS data. Finally, we briefly report on a investigation of the possible existence of pulsating warm ($T_{\rm eff} \sim 19\,000$ K) DA white dwarfs, and the null results from TESS.

3.1. *Outbursting ZZ Ceti stars*

The *Kepler* spacecraft observations of ZZ Ceti stars revealed a new type of phenomenon never observed before from the ground: outburst-like events in DAV stars (Bell et al. 2017). The first one, WD J1916+3938 (KIC4552982), was observed during 1.5 years. 20 pulsation modes with periods typical of ZZ Ceti stars were detected, along with 178 enhancements of brightness typical of outburst phenomena, with peaks of up to 17 % above the quiescent level, involving very energetic events ($E \sim 10^{33}$ erg), with

a mean recurrence period of about 2.7 days (Bell et al. 2015). The second outbursting ZZ Ceti star, PG1149+057, was studied by Hermes et al. (2015). This star shows flux enhancements of up to 45% above the quiescent level! It was revealed that for this star, the outbursts actually affect the normal pulsations (in amplitude and frequency). This leads to the important conclusion that outbursts are an intrinsic phenomenon of the (otherwise isolated) star. At present, a total of 8 outbursting isolated ZZ Ceti stars have been discovered (Bell et al. 2016, 2017), close to the red edge of the ZZ Ceti instability strip. A possible explanation is connected with parametric instability via mode coupling of white dwarf pulsations (Dziembowski 1982; Wu, & Goldreich 2001; Luan, & Goldreich 2018).

3.2. *Dichotomy of mode line widths in ZZ Ceti stars*

Hermes et al. (2017) discovered a dichotomy of mode line widths in the power spectrum of pulsating DA white dwarfs observed from space. Specifically, low-frequency modes with periods longer than roughly 800 s are generally incoherent over the length of observations, while higher-frequency modes ($<$ 800 s) are observed to be much more stable in phase and amplitude. This phenomenon is incompatible with stochastic excitation, that for white dwarfs would be able to excite pulsations with periods of the order of $\sim$ 1 sec. 27 DAVs were observed through K2 Campaign by the *Kepler* space telescope in the study of Hermes et al. (2017). The dichotomy of model line width can be related to the oscillation of the outer convection zone of a DA white dwarfs during pulsations. The oscillation of the base of the outer convection zone would affect g-mode eigenfunctions having the outer turning point located at the base of the convection zone (Montgomery et al. 2019). Deepening the study of this phenomenon can lead to a better understanding of the properties of the outer convection zone of DA white dwarfs.

3.3. *White-dwarf rotation rates from asteroseismology*

The rotation rates of 27 isolated DA white dwarfs have been determined via asteroseismology using rotational splittings by Hermes et al. (2017) with observations from *Kepler*/K2 Mission. In this way, the number of pulsating white dwarfs with measured rotation rates has been doubled (see Table 10 of Córsico et al. 2019a). The results indicate that the mean rotation period is of $\sim 30 - 40$ hours, although fast rotating stars have also been found, with periods of $\sim 1 - 2$ hours. Evidence has been found for a link between high mass and fast rotation, although additional massive white dwarfs are required to confirm this trend. If true, this trend would favor the hypothesis that the high-mass white dwarfs are the result of mergers, which are supposed to rotate very fast. Hermes et al. (2017) find that the majority of isolated descendants of $1.73.0 M_{\odot}$ ZAMS progenitors rotate at $\sim$ 1.5 days, instead of minutes! This indicates that most internal angular momentum must be lost on the first-ascent giant branch.

3.4. *Amplitude and frequency variations of g modes in a DBV white dwarf*

By using observations from the *Kepler* mission, Zong et al. (2016a) have detected amplitude and frequency variations of the components of the triplets of frequencies caused by rotation in the DBV star KIC 08626021. The timescale for the quasi-periodic modulations of the variations is of about 600 days, undetectable from ground-based observations. A similar phenomenon has been detected with *Kepler* in the pulsating sdB star KIC 10139564 (Zong et al. 2016b). It is thought that the modulations of frequencies and amplitudes are not related to any evolutionary effect (e.g., neutrino cooling), since the timescales involved are several orders of magnitude shorter than the cooling rate of DB white dwarfs. These modulations cannot be attributed to signatures of orbiting com-

panions around the star, because different timescales for different triplets are detected. Therefore, a possible explanation is nonlinear resonant mode coupling in rotationally split triplets (Buchler et al. 1997; Goupil et al. 1998). If so, this star could constitute a new window to study nonlinear pulsations. On the other hand, the detected frequency modulations can potentially prevent a measurement of the evolutionary (cooling) rate of period change of the star.

3.5. *The DBV pulsator WD0158−160: TESS observations*

The first pulsating white dwarf analyzed with TESS is the DBV pulsator WD0158−160 (also called EC01585−1600, G272−B2A, TIC257459955; Bell et al. 2019). TESS performs extensive time-series photometry that allows to discover pulsating stars, and, in particular, pulsating white dwarfs. The TESS Asteroseismic Science Consortium (TASC) Working Group 8 (WG8) focuses on TESS observations of evolved compact stars that exhibit photometric variability, including hot subdwarfs, white dwarfs, and pre-white dwarfs with mag < 16, with short (120 sec) cadence. TIC257459955 is a known DBV white dwarf with $T_{\rm eff} = 24\,100$ K and $\log g = 7.88$ (Rolland et al. 2018), or alternatively, $T_{\rm eff} = 25\,500$ K and $\log g = 7.94$ (Voss et al. 2007). Bell et al. (2019) find 9 independent frequencies suitable for asteroseismology plus frequency combinations. The periods of genuine eigenmodes are in the range $[245 - 866]$ sec, with a period spacing of $\Delta\Pi = 38.1 \pm 1.0$ s associated to $\ell = 1$. The comparison with the average of the computed period spacings (see Section 2.3.1) gives an estimate of the stellar mass. Here, it is assumed that the period spacing is primarily dependent on $T_{\rm eff}$ and $M_\star$ (and very weakly on $M_{\rm He}$). This method indicates a stellar mass of $M_\star = 0.621 \pm 0.06 M_\odot$, or alternatively, $M_\star = 0.658 \pm 0.10 M_\odot$ (according to the two different spetroscopic determinations of $T_{\rm eff}$), larger than the spectroscopic estimates ($M_\star = 0.542 - 0.557 M_\odot$). The star also has been analyzed by performing period-to-period fits (Section 2.3.2) by employing a fully evolutionary model approach (La Plata Group) and a parametric approach (Texas Group). There exist families of asteroseismic solutions, but the solution that satisfies the spectroscopic parameters and the astrometric constraints from Gaia, is characterized by a DB white dwarf model with $M_\star \sim 0.60 M_\odot$, $T_{\rm eff} \sim 25\,600$ K, $M_{\rm He} \sim 3 \times 10^{-2} M_\star$, $d \sim 67$ pc, and a rotation period of ~ 7 or ~ 14 hours. It is worth emphasizing that the asteroseismological solutions from the La Plata Group and the Texas Group are similar regarding the location of the chemical transition zones, which are mainly responsible for setting the period spectrum of a white dwarf model.

3.6. *The possible existence of pulsating warm DA white dwarfs*

In their theoretical pioneering work, Winget et al. (1982) (see also Winget 1982) predicted the possible existence of warm ($T_{\rm eff} \sim 19\,000$ K) pulsating DA white-dwarf stars, hotter than ZZ Ceti stars. However, to date, no pulsating warm DA white dwarf has been detected. Althaus et al. (2019) re-examined the pulsational predictions for such white dwarfs on the basis of new full evolutionary sequences and also analyzed a sample of warm DA white dwarfs observed by the TESS satellite in order to search for the possible pulsational signals. Althaus et al. (2019) computed white-dwarf evolutionary sequences with very small H content, appropriate for the study of warm DA white dwarfs, employing a new full-implicit treatment of time-dependent element diffusion. Also, they computed non-adiabatic pulsations in the effective temperature range of $30\,000 - 10\,000$ K, focusing on $\ell = 1$ g modes with periods in the range $50 - 1500$ s. These authors found that extended and smooth He/H transition zones inhibit the excitation of g modes due to partial ionization of He below the H envelope, and only in the case that the H/He transition is assumed to be much more abrupt, do the models exhibit pulsational instability.

In this case, instabilities are found only in white dwarf models with H envelopes in the range of $-14.5 \lesssim \log(M_{\rm H}/M_\star) \lesssim -10$ and at effective temperatures higher than those typical of ZZ Ceti stars, in agreement with the previous study by Winget et al. (1982). Althaus et al. (2019) found that none of the warm DAs observed by the TESS satellite are pulsating. This study suggests that the non-detection of pulsating warm DA white dwarfs, if white dwarfs with very thin H envelopes do exist, could be attributed to the presence of a smooth and extended H/He transition zone. This could be considered as an indirect proof that element diffusion indeed operates in the interior of white dwarfs.

4. Conclusions

From the beginning to the present, white-dwarf asteroseismology has undergone impressive progress, in recent years by the availability of space missions that provide unprecedented high-quality data, but also from ground-based observations, mainly with the spectral observations of the Sloan Digital Sky Survey (SDSS, York et al. 2000). This progress from the observational front has been accompanied by the development of new detailed models of white dwarf stars and novel implementations of asteroseismological techniques. The combination of these factors is leading the white-dwarf asteroseismologists to realize the desire to know the details of the inner structure and evolutionary origins of these stars. These studies will soon be driven by new observations from space (TESS, PLATO, Cheops). Therefore, the future of this area is, at the very least, very promising.

Acknowledgements

I would warmly thanks the Local Organising Committee of the IAU Symposium 357, in particular to Professor Martin Barstow, for support that allowed me to attend this conference.

References

Althaus, L. G., Córsico, A. H., Isern, J., García-Berro, E. 2010, A&ARv,18, 471
Althaus, L. G., Miller Bertolami, M. M., & Córsico, A. H. 2013, A&A, 557, A19
Althaus, L. G., Córsico, A. H., Uzundag, M., et al. 2019, arXiv e-prints, arXiv:1911.02442
Baglin, A. 1969, Astrophysical Letters, 3, 119
Baglin, A., Auvergne, M., Barge, P., et al. 2009, Transiting Planets, 71
Bell, K. J., Córsico, A. H., Bischoff-Kim, A., et al. 2019, A&A, 632, A42
Bell, K. J., Hermes, J. J., Montgomery, M. H., et al. 2017, 20th European White Dwarf Workshop, 303
Bell, K. J., Hermes, J. J., Montgomery, M. H., et al. 2016, ApJ, 829, 82
Bell, K. J., Hermes, J. J., Bischoff-Kim, A., et al. 2015, ApJ, 809, 14
Bergeron, P., Wesemael, F., Dufour, P., et al. 2011, ApJ, 737, 28
Borucki, W. J., Koch, D., Basri, G., et al. 2010, Science, 327, 977
Buchler, J. R., Goupil, M.-J., & Hansen, C. J. 1997, A&A, 321, 159
Camisassa, M. E., Althaus, L. G., Córsico, A. H., et al. 2019, A&A, 625, A87
Chanmugam, G. 1972, Nature Physical Science, 236, 83
Moya, A., Barceló Forteza, S., Bonfanti, A., et al. 2018, A&A, 620, A203
Córsico, A. H., De Gerónimo, F. C., Camisassa, M. E., et al. 2019, arXiv e-prints, arXiv:1910.07385
Córsico, A. H., Althaus, L. G., Miller Bertolami, M. M., et al. 2019, A&ARv, 27, 7
Córsico, A. H., Althaus, L. G., Miller Bertolami, M. M., et al. 2012, A&A, 541, A42
Córsico, A. H., Althaus, L. G., Miller Bertolami, M. M., et al. 2009, A&A, 499, 257
Córsico, A. H., Althaus, L. G., Kepler, S. O., et al. 2008, A&A, 478, 869

Córsico, A. H., Althaus, L. G., Miller Bertolami, M. M., et al. 2007, A&A, 461, 1095
Córsico, A. H., Miller Bertolami, M. M., Althaus, L. G., et al. 2007, A&A, 475, 619
Dziembowski, W. 1982, Acta. Astron., 32, 147
Faulkner, J., & Gribbin, J. R. 1968, Nature, 218, 734
Fontaine, G., Brassard, P. 2008 PASP, 120, 1043
García-Berro, E., Torres, S., Althaus, L. G., et al. 2010, Nature, 465, 194
Goupil, M. J., Dziembowski, W. A., & Fontaine, G. 1998, Baltic Astronomy, 7, 21
Harper, R. V. R., & Rose, W. K. 1970, ApJ, 162, 963
Hermes, J. J., Gänsicke, B. T., Kawaler, S. D., et al. 2017, ApJS, 232, 23
Hermes, J. J., Montgomery, M. H., Bell, K. J., et al. 2015, ApJL, 810, L5
Howell, S. B., Sobeck, C., Haas, M., et al. 2014, PASP, 126, 398
Kawaler, S. D., & Bradley, P. A. 1994, ApJ, 427, 415
Koen, C., & Laney, D. 2000, MNRAS, 311, 636
Landolt, A. U. 1968, ApJ, 153, 151
Lasker, B. M., & Hesser, J. E. 1969, ApJL, 158, L171
Lasker, B. M., & Hesser, J. E. 1971, ApJL, 163, L89
Ledoux, P. J., & Sauvenier-Goffin, E. 1950, ApJ, 111, 611
Luan, J., & Goldreich, P. 2018, ApJ, 863, 82
McGraw, J. T. 1979, ApJ, 229, 203
Mestel, L. 1952, MNRAS, 112, 583
Miller Bertolami, M. M., & Althaus, L. G. 2006, A&A, 454, 845
Montgomery, M. H., Hermes, J. J., & Winget, D. E. 2019, arXiv e-prints, arXiv:1902.05615
Ostriker, J. P., & Tassoul, J.-L. 1968, Nature, 219, 577
Piotto, G. 2018, European Planetary Science Congress, EPSC2018-969
Ricker, G. R., Winn, J. N., Vanderspek, R., et al. 2015, Journal of Astronomical Telescopes, Instruments, and Systems, 1, 014003
Robinson, E. L., Nather, R. E., & McGraw, J. T. 1976, ApJ, 210, 211
Robinson, E. L., Kepler, S. O., & Nather, R. E. 1982, ApJ, 259, 219
Rolland, B., Bergeron, P., & Fontaine, G. 2018, ApJ, 857, 56
Sauvenier-Goffin, E. 1949, Annales d'Astrophysique, 12, 39
Tassoul, M., Fontaine, G., & Winget, D. E. 1990, ApJS, 72, 335
Unno, W., Osaki, Y., Ando, H., et al. 1989, Nonradial oscillations of stars
Voss, B., Koester, D., Napiwotzki, R., et al. 2007, A&A, 470, 1079
Walker, G., Matthews, J., Kuschnig, R., et al. 2003, PASP, 115, 1023
Warner, B., & Robinson, E. L. 1972, Nature Physical Science, 239, 2
Winget, D. E., Kepler, S. O. 2008, ARAA 46,157
Winget, D. E., van Horn, H. M., Tassoul, M., et al. 1982, ApJL, 252, L65
Winget, D. E. 1982, Ph.D. Thesis
Wu, Y., & Goldreich, P. 2001, ApJ, 546, 469
York, D. G., Adelman, J., Anderson, J. E., et al. 2000, AJ, 120, 1579
Zong, W., Charpinet, S., Vauclair, G., et al. 2016, A&A, 585, A22
Zong, W., Charpinet, S., & Vauclair, G. 2016, A&A, 594, A46